International Journal of Nanomedicine

Dovepress
open access to scientific and medical research

Open Access Full Text Article

ORIGINAL RESEARCH

Comparative proteomics of inhaled silver nanoparticles in healthy and allergen provoked mice

This article was published in the following Dove Press journal:
International Journal of Nanomedicine
2 August 2013
Number of times this article has been viewed

Chien-Ling Su[1,2]
Tzu-Tao Chen[1,3]
Chih-Cheng Chang[1,3]
Kai-Jen Chuang[4,5]
Cheng-Kuan Wu[6]
Wen-Te Liu[1,2]
Kin Fai Ho[7]
Kang-Yun Lee[1,8]
Shu-Chuan Ho[2,8]
Hsiu-Er Tseng[9]
Hsiao-Chi Chuang[1,2]
Tsun-Jen Cheng[6,10]

On behalf of the Taiwan CardioPulmonary Research Group (T-CPR)

[1]Division of Pulmonary Medicine, Department of Internal Medicine, Shuang Ho Hospital, [2]School of Respiratory Therapy, College of Medicine, [3]Graduate Institute of Clinical Medicine, College of Medicine, [4]Department of Public Health, School of Medicine, College of Medicine, [5]School of Public Health, College of Public Health and Nutrition, Taipei Medical University, [6]Institute of Occupational Medicine and Industrial Hygiene, College of Public Health, National Taiwan University, Taipei, Taiwan; [7]School of Public Health and Primary Care, The Chinese University of Hong Kong, Hong Kong, People's Republic of China; [8]Department of Thoracic Medicine, Chang Gung Memorial Hospital, Chang Gung University College of Medicine, [9]Division of Consultation and Promotion, Taiwan Drug Relief Foundation, [10]Department of Public Health, College of Public Health, National Taiwan University, Taipei, Taiwan

Correspondence: Hsiao-Chi Chuang
School of Respiratory Therapy, College of Medicine, Taipei Medical University, Taipei, Taiwan
Tel +886 2 2736 1661 ext 3515
Fax +886 2 2739 1143
Email r92841005@ntu.edu.tw

Tsun-Jen Cheng
Institute of Occupational Medicine and Industrial Hygiene and Department of Public Health, College of Public Health, National Taiwan University, Taipei, Taiwan
Tel +886 2 3366 8090
Fax +886 2 2395 7845
Email tcheng@ntu.edu.tw

Background: Silver nanoparticles (AgNPs) have been associated with the exacerbation of asthma; however, the immunological basis for the adjuvant effects of AgNPs is not well understood.

Objective: The aim of the study reported here was to investigate the allergic effects of AgNP inhalation using proteomic approaches.

Methods: Allergen provoked mice were exposed to 33 nm AgNPs at 3.3 mg/m^3. Following this, bronchoalveolar lavage fluid (BALF) and plasma were collected to determine protein profiles.

Results: In total, 106 and 79 AgNP-unique proteins were identified in the BALF of control and allergic mice, respectively. Additionally, 40 and 26 AgNP-unique proteins were found in the plasma of control and allergic mice, respectively. The BALF and plasma protein profiles suggested that metabolic, cellular, and immune system processes were associated with pulmonary exposure to AgNPs. In addition, we observed 18 proteins associated with systemic lupus erythematosus that were commonly expressed in both control and allergic mice after AgNP exposure. Significant allergy responses were observed after AgNP exposure in control and allergic mice, as determined by ovalbumin-specific immunoglobulin E.

Conclusion: Inhaled AgNPs may regulate immune responses in the lungs of both control and allergic mice. Our results suggest that immunology is a vital response to AgNPs.

Keywords: bronchoalveolar lavage, immunotoxicology, proteome, systemic lupus erythematosus, serum

Introduction

Silver nanoparticles (AgNPs) are clusters of silver atoms with at least one dimension measuring <100 nm. AgNPs have antibacterial and antimicrobial properties that are advantageous for applications in medicine. Therefore, AgNPs are increasingly utilized substrates that have been highly commercialized. For example, clothing industries have added AgNPs into fabrics used to make socks, exploiting the antibacterial activity to neutralize odor-forming bacteria.[1] AgNPs have also been integrated into plastics and surface coatings. Recently, AgNPs have been investigated for treating asthma;[2,3] however, the effects of AgNP inhalation on healthy and asthmatic individuals are unclear.

The potential for nanomedicine in allergen immunotherapy is currently being investigated and developed. AgNPs are candidates for the treatment of allergic asthma.[2,3] AgNPs have larger surface area-to-volume ratios for interacting with bacteria and lower toxicity than other metal nanoparticles (NPs).[4] A recent study of the immunology of AgNPs suggested that they have significant adjuvant effects and

that the mechanism of these effects is the recruitment and activation of local leukocytes, especially macrophages.[5] Park et al observed that AgNPs might have an antioxidant effect by attenuating antigen-induced airway inflammation and hyperresponsiveness.[2] Further, AgNPs suppressed mucus hypersecretion and the vascular endothelial growth factor signaling pathway during allergic airway inflammation.[3] However, biological applications employing AgNPs should be thoroughly studied for potential negative side effects.[6,7]

Toxicoproteomics is increasingly applied to discover diagnostic biomarkers of human disease, for example, lung cancer.[8] A "protein biomarker" is a protein or peptide that can be objectively and quantitatively measured and evaluated as an indicator of normal or pathological biological processes, exposure to environmental factors, lifestyle factors, the presence of pathogens, or responsiveness to a therapeutic intervention. In this regard, bronchoalveolar lavage fluid (BALF) and blood samples may be used to measure biomarkers for several purposes, including diagnosis, screening, evaluation of risk or predisposition, assessment of prognosis, or surrogate markers.[9] Several techniques have been developed for proteomic research. For example, two-dimensional gel electrophoresis is commonly used to identify unique protein expression profiles in biological samples. Mass spectrometry for protein identification has been successfully utilized in a number of toxicology studies. Further, gas-phase fractionation is an iterative mass spectrometry approach that examines multiple smaller mass-to-charge ranges. This process enables the ions selected for collision-induced dissociation to come from a greater number of unique peptides compared with the ions selected from the wide mass range scan in automated liquid chromatography-tandem mass spectrometry analysis.[10,11] Proteomics approaches are becoming more popular in clinical medicine and environmental toxicology.

Inflammation, thrombosis and coagulation, and vascular function and heart rate variability are the human pathophysiological responses to particulate pollution exposure.[12] However, there is no standard guidance for AgNP inhalation exposure. Nonetheless, the protein profiles in body fluids and their biological pathways following AgNP exposure remain unclear. The objective of this study was to investigate the protein profiles and potential biological pathway in biological fluids in healthy and allergic subjects using proteomic analyses. We established an ovalbumin (OVA)-sensitized allergic mouse model to evaluate the allergenicity of AgNPs in healthy and susceptible mice. The animals inhaled AgNPs that were generated by an evaporation–condensation method. After AgNP inhalation, the BALF and plasma protein profiles were identified in allergic and healthy mice. Finally, we analyzed the biological processes, protein functional classifications, and pathways based on the identified proteins.

Materials and methods

Animals

Female 6-week-old BALB/c mice were obtained from BiOLASCO (Taipei, Taiwan). The mice were maintained at a constant temperature and a relative humidity of 22°C ± 2°C and 55% ± 10%, respectively; a light–dark cycle (12–12 hours) was used throughout the study. The animals were housed in plastic cages and were provided the Lab Diet 5001 (PMI Nutrition International, St Louis, MO, USA) and water ad libitum during acclimatization and pre- and post-exposure. The animal experiments were performed in compliance with the animal and ethics review committee of the Laboratory Animal Centre at the National Taiwan University (Taipei, Taiwan).

AgNP generation and characterization

An evaporation–condensation method was used to generate AgNPs, as described previously.[13,14] In brief, silver powder (>99%, Merck KGaA, Darmstadt, Germany) was evaporated at the centre of a 1,100°C tube furnace (model T11-301, SJ Ltd, Taipei, Taiwan), and the generated silver vapor was transported continuously using nitrogen at a flow rate of 6 L/minutes. Because the furnace outlets were equipped with a chilling system, the silver vapor was quenched suddenly and condensed to form AgNPs. In this study, an additional condition section was introduced between the generation system and the exposure chamber to guarantee that the temperature, relative humidity, and composition of the exposed AgNP stream were close to the constant environmental conditions. The oxygen and nitrogen air (5 L/minute at a flow rate of 1:1) was delivered and mixed with the exposed AgNP stream. Next, the exposed AgNP stream was split into two routes for filtration with or without high-efficiency particulate air filters before its introduction into whole-body exposure chambers, which have been described previously.[15]

A TSI Scanning Mobility Particle Sizer™ Spectrometer 3936 with nano-differential mobility analyzer (DMA) (TSI Incorporated, Shoreview, MN, USA) was used to continuously monitor the size distribution of AgNPs in the exposure chamber throughout the entire exposure period. The flow rates of the aerosol stream and sheath air of the

scanning mobility particle sizer were fixed at 0.3 and 3.0 L/minute, respectively. The scanning mobility particle sizer was calibrated with 100 nm National Institute of Standards and Technology-traceable polystyrene latex spheres standard particles before the experiment. The total particle number concentrations, the number-based geometric mean diameter, and the geometric standard deviation were recorded. To physicochemically characterize the generated AgNPs, AgNPs were collected onto 37 mm Teflon substrates (Merck Millipore, Darmstadt, Germany), quarters of which were fixed onto 13 mm aluminum scanning electron microscopy (SEM) stubs.[16] The samples were platinum-coated to an average thickness of 10 nm using a sputter coater and were imaged using an Inspect™ SEM (FEI, Hillsboro, OR, USA) at an accelerating voltage of 3 kV and a spot size of 2.5.

Inductively coupled plasma mass spectrometry (ICP-MS; Elan 500, PerkinElmer, Waltham, MA, USA) was used to determine any contamination in the AgNPs. These samples were digested with concentrated nitric acid (Fisher Primar grade, specific gravity 1.48; Thermo Fisher Scientific, Waltham, MA, USA) carried out in a CEM MDS-2000 microwave digestor oven (CEM, SpectraLab Scientific Inc, Markham, ON, Canada), using CEM advanced Teflon-lined composite vessels.[17] The pressure was increased to 80 pounds per square inch for approximately 20 minutes, producing a digestion temperature of approximately 180°C. Samples were diluted to 10% nitric acid using deionized (>18 MΩ) water. Nitric acid blanks were run to detect any contamination during the analysis process. A solution of a certified rock standard (BCR1) was used to check the accuracy of the analyses.

Allergic sensitization, AgNP inhalation, and OVA challenge

To assess the allergenicity of AgNPs, we used endotoxin-free OVA (Sigma-Aldrich, St Louis, MO, USA) as an allergen to induce systemic sensitization. The procedure used to develop allergic airway disease in mice after AgNP exposure was modified from a published method.[18] The experimental design is shown in Figure 1. Mice were divided into four groups (control groups 1 and 2 and allergy groups 3 and 4 [OVA]). Group 1 and 3 mice were exposed to high-efficiency particulate air filtered air (FA; n = 5 each group), whereas Group 2 and 4 were exposed to AgNPs (n = 6 each group). On Day 0, the mice in the allergic groups received an intraperitoneal injection of 50 µg OVA in aluminum hydroxide adjuvant prepared in phosphate-buffered saline (PBS), whereas those in the control groups received the same volume of adjuvant prepared in PBS alone. On Day 8,

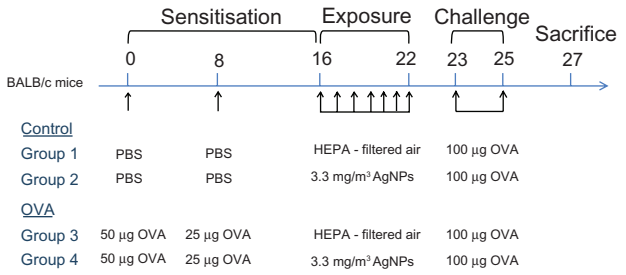

Figure 1 Experimental design for investigating the effects of silver nanoparticles (AgNPs) on the allergic response to ovalbumin (OVA) antigen using proteomic approaches. OVA: OVA in aluminum hydroxide adjuvant prepared in phosphate-buffered saline (PBS); PBS (control): aluminum hydroxide adjuvant prepared in PBS.
Abbreviation: HEPA, high-efficiency particulate air.

the mice in the allergic groups received an intraperitoneal injection of 25 µg OVA in aluminum hydroxide adjuvant prepared in PBS, whereas the control groups received the same volume of adjuvant prepared in PBS alone. The mice in the control groups demonstrated a significantly lower level of OVA-specific immunoglobulin (Ig) E than the mice sensitized with OVA ($P < 0.001$). On Day 16, the allergic and control mice were exposed to 33 nm AgNPs (3.3 ± 0.7 mg/m^3; Groups 2 and 4) and FA (Groups 1 and 3) in the whole-body chambers for 7 days (6 hours/day, from Day 16 to 22). The mice were challenged intranasally with 100 µg OVA between Days 23 and 25, and the animals were euthanized on Day 27.

Animal necropsy and sample collection

Animal necropsy, and BALF and blood collections were performed as described previously.[19] Facial vein blood collection was performed before euthanasia. For BALF collection, animals were euthanized with a single intraperitoneal injection of sodium pentobarbitone (200 mg/mL). A single 0.1 mL volume of PBS was used to lavage the lungs. All samples were centrifuged at $1,500 \times g$ for 5 minutes at 4°C and the cell pellet was removed. For proteomic analyses, 0.5 mL of BALF or a plasma sample from each group was pooled together following protein preparation.

Trichloroacetic acid precipitation

The BALF samples were diluted in 120 µL dd-H_2O, dried with a SpeedVac concentrator (Thermo Scientific, Asheville, NC, USA), denatured and reduced with 1% sodium dodecyl sulfate/10 mM dithiothreitol (Sigma-Aldrich) at 95°C for 5 minutes and alkylated with 50 mM iodoacetamide (Sigma-Aldrich) in the dark at room temperature for 30 minutes. Trichloroacetic acid (Sigma-Aldrich) was added to a final concentration of 20%. The mixture was incubated for

15 minutes on ice and then centrifuged at 13,000 rpm for 10 minutes. The supernatant was removed. The pellet was washed once with 10% trichloroacetic acid and three times with dd-H_2O then it was centrifuged at 13,000 rpm for another 5 minutes. Again the supernatant was removed, and then the pellet was digested with trypsin in 25 mM ammonium bicarbonate (Sigma-Aldrich) at 37°C for 18 hours.

Protein digestion

Plasma samples (2.5 µL) were diluted to 1 mL with 50 mM ammonium bicarbonate. Samples were denatured and reduced with 8 M urea/10 mM dithiothreitol at 37°C for 1 hour and alkylated with 50 mM iodoacetamide in the dark at room temperature for 30 minutes. Samples were digested with trypsin in 25 mM ammonium bicarbonate at 37°C for 18 hours and then desalted using C18 columns.

Mass spectrometry and protein identification

The tryptic peptides were analyzed with a Q Exactive mass spectrometer (Thermo Fisher Scientific) coupled with a Dionex UltiMate® 3000 Rapid Separation LC system (Thermo Fisher Scientific). Peptide separation was performed by liquid chromatography with C18 columns (Dionex Acclaim® PepMap™ RSLC, 75 × 150 mm, 2 µm; Thermo Fisher Scientific) with the following conditions: linear gradient from 1% to 40% of Mobile phase B (Mobile phase A: 5.0% acetonitrile/0.1% formic acid, Mobile phase B: 95.0% acetonitrile/0.1% formic acid) for 55 minutes and then 40%–90% of Mobile phase B for 5 minutes, with a 90-minute separation time. Full mass spectrometry (MS) scans were performed with ranges of *m/z* 380–2,000, *m/z* 380–600, *m/z* 600–800, *m/z* 800–1,200, and *m/z* 1,200–2,000, and the ten most intense ions from MS scans were selected for MS/MS scans. Raw data were processed into peak lists by Proteome Discoverer (v 1.3; Thermo Scientific) for Mascot database search (http://www.matrixscience.com/search_form_select.html) with the National Centre for Biotechnology Information and UniProt database prediction and literature search. Search parameters included variable modifications for deamidation (NQ), oxidation (M), and fixed modification for carbamidomethyl (C). The maximum mass tolerance was set to 10 ppm for precursor ions and 0.05 Da for fragment ions.

Protein functional analyses

The expressed BALF and plasma proteins (Group 1 vs Group 3 and Group 2 vs Group 4) were analyzed with the Protein ANalysis THrough Evolutionary Relationships (PANTHER) Classification System (http://www.pantherdb.org/) and the Database for Annotation, Visualization and Integrated Discovery (DAVID) gene functional analysis tools (http://david.abcc.ncifcrf.gov/) to better understand the biological context of the identified proteins, their connection to disease pathology, and their participation in physiological pathways.[20,21] The UniProt accession database was used to access the 19 overlapping BALF proteins (between Group 1 vs Group 3 and Group 2 vs Group 4) identified in this study. These proteins were uploaded and mapped against the Mus musculus reference dataset to extract and summarize the functional annotation associated with individual genes/proteins or groups of genes/proteins and to identify the gene ontology terms, biological processes, functional classification, and important pathways for each dataset.

Determination of OVA-specific IgE

The plasma OVA-specific IgE levels before (on Day 15) and after (on Day 23) AgNP exposure and OVA challenge were measured using Mouse IgE ELISA Set (BD Biosciences San Jose, CA, USA) in accordance with the manufacturer's instructions.

Results

Characterization of AgNPs

AgNPs were generated by the evaporation–condensation method and were physicochemically characterized by SEM. Spherical AgNPs with an average size of 33 nm and a total mass of 3.3 ± 0.7 mg/m^3 were produced, and the vast majority of these rapidly aggregated to form clusters (Figure 2). ICP-MS data from filters with and without AgNPs demonstrated the production of Ag-containing NPs. The ICP-MS results also excluded the possibility of impurities or contaminants introduced to the AgNPs during their generation.

Proteomic profile of BALF

To identify the proteins expressed after AgNP exposure, the overlaps in protein profiles between FA and AgNP inhalation in control (Figure 3A) and allergy groups were compared (Figure 3A). There were 169 proteins identified in FA-exposed control mice, whereas 220 proteins were determined in AgNP-exposed control mice. There were 114 common proteins in control mice exposed to FA or AgNP. Therefore, 55 and 106 proteins were unique for FA and AgNP, respectively. We further analyzed the 106 unique AgNP-associated proteins in the control BALF

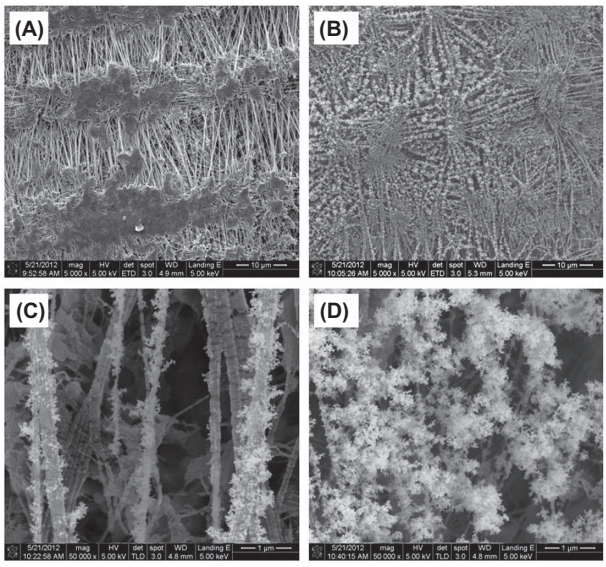

Figure 2 Scanning electron microscopy images of (**A**) the blank Teflon substrate and (**B**) silver nanoparticles (AgNPs) collected on the Teflon substrate at 5,000× and (**C** and **D**) 50,000× magnification.

samples (Table S1). Similarly, 151 and 211 proteins were identified in allergic mice after FA and AgNP exposure, respectively. Because there were 132 common proteins expressed after FA or AgNP exposure, there were 19 and 79 proteins unique to FA and AgNP exposure, respectively.

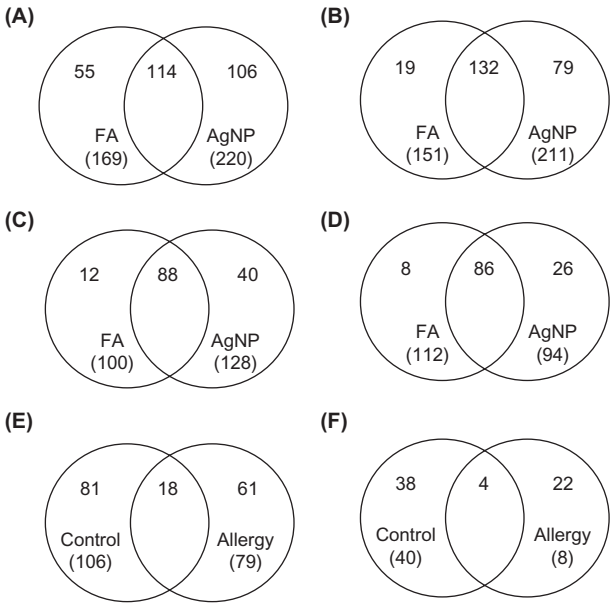

Figure 3 Venn diagrams showing the proteins common or unique to silver nanoparticle (AgNP) treatment. (**A**) Bronchoalveolar lavage fluid (BALF) proteins in control mice, (**B**) BALF proteins in allergic mice, (**C**) plasma proteins in control mice, and (**D**) plasma proteins in allergic mice. The identified AgNP-unique proteins were further analyzed for commonalities in control and allergic mice after AgNP exposure. (**E**) Proteins commonly expressed in BALF and (**F**) proteins commonly expressed in plasma.

Abbreviation: FA, filtered air.

The 79 unique AgNP-associated proteins in the allergic BALF samples were further analyzed (Table S2).

MS-based functional pathway analyses were performed with the BALF proteins in control and allergy groups to understand their biological context. PANTHER analysis was initially used to examine the protein functions in biological processes (Figure 4). These proteins were associated with 15 biological processes (Figure 4A): cell communication (11.4% for control and 10.2% for allergy), cellular processes (15.7% for control and 14.1% for allergy), transport (5.0% for control and 9.4% for allergy), cellular component organization (4.3% for control and 5.5% for allergy), apoptosis (0.7% for control and 3.1% for allergy), system processes (5.7% for control and 4.7% for allergy), stimulus response (9.3% for control and 7.8% for allergy), developmental processes (8.6% for control and 8.6% for allergy), metabolic processes (18.6% for control and 17.2% for allergy), cell cycle (2.1% for control and 3.9% for allergy), immune system processes (11.4% for control and 10.9% for allergy), cell adhesion (3.6% for control and 4.7% for allergy), reproduction (1.4% for control only), homeostatic processes (0.7% for control only), and the generation of precursor metabolites and energy (1.4% for control only). Metabolic, cellular, and immune system processes and cell communication were the critical biological processes that were modulated in response to AgNP exposure in both control and allergic mice, as determined by BALF analysis.

Functional pathways were further investigated using PANTHER analysis (Figure 5). The AgNP-unique proteins in the control and allergy groups were involved in 12 pathways, including those mediating blood coagulation, integrin signaling, ubiquitin proteasomes, inflammation resulting from chemokine and cytokine signaling, T-cell activation, tricarboxylic acid cycle, dopamine receptor-mediated signaling, plasminogen activating cascade, Fas signaling pathway, cytoskeletal regulation by Rho GTPase, nicotine pharmacodynamics, and nicotinic acetylcholine receptor signaling.

Proteomic profile of plasma

The protein profiles in plasma after FA and AgNP inhalation by control (Figure 3C) or allergy groups were compared (Figure 3D). We identified 100 proteins expressed in FA-exposed control mice and 128 in AgNP-exposed control mice; there were 88 proteins common to both control exposures. There were 12 and 40 proteins unique to FA and AgNP, respectively. We used the 40 unique AgNP-associated proteins in the control BALF samples for further

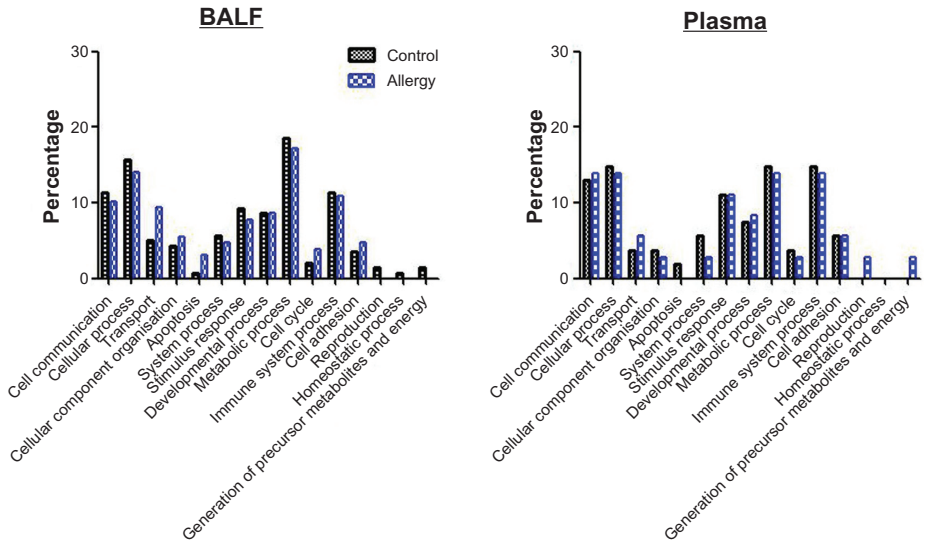

Figure 4 Biological process in (**A**) bronchoalveolar lavage fluid (BALF) and (**B**) plasma obtained using Protein ANalysis THrough Evolutionary Relationships (PANTHER) analysis.

analyses (Table S3). Additionally, there were 112 and 94 proteins identified in allergic mice after FA or AgNP exposure, respectively, 86 of which were shared by both groups. There were eight and 26 proteins uniquely expressed after FA and AgNP exposure, respectively. The 26 unique AgNP-associated proteins in the allergic BALF samples were further analyzed (Table S4).

PANTHER analysis was used to examine the protein functions in biological processes (Figure 4). These proteins were associated with 14 biological processes (Figure 4B): cell communication (13.0% for control and 13.9% for allergy), cellular processes (14.8% for control and 13.9% for allergy), transport (3.7% for control and 5.6% for allergy), cellular component organization (3.7% for control and 2.8% for allergy), apoptosis (1.9% for control only), system processes (5.6% for control and 2.8% for allergy), stimulus response (11.1% for control and 11.1% for allergy), developmental processes (7.4% for control and 8.3% for allergy), metabolic processes (14.8% for control and 13.9% for allergy), cell cycle (3.7% for control and 2.8% for allergy), immune system processes (14.8% for control and 13.9% for allergy), cell adhesion (5.6% for control and 5.6% for allergy), reproduction (2.8% for allergy only) and the generation of precursor metabolites and energy (2.8% for

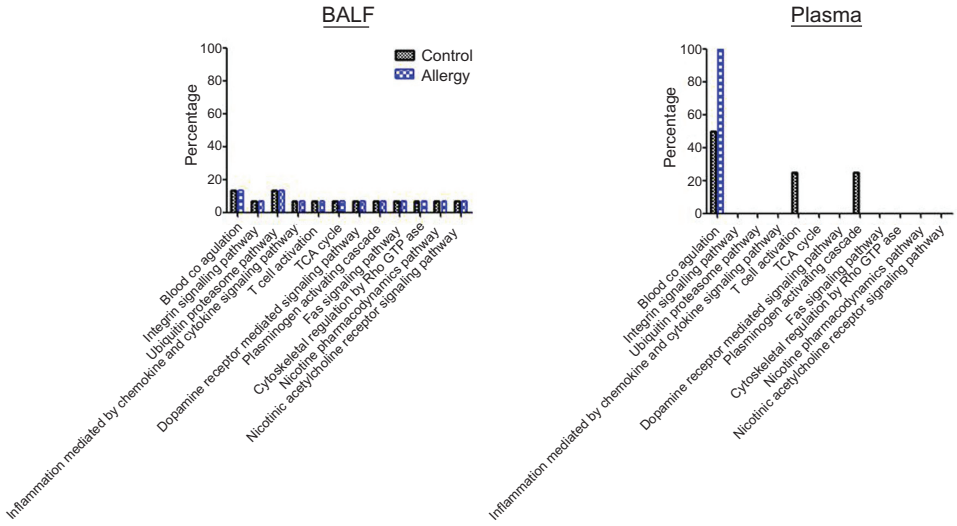

Figure 5 Pathway analysis in (**A**) bronchoalveolar lavage fluid (BALF) and (**B**) plasma protein using Protein ANalysis THrough Evolutionary Relationships (PANTHER) analysis.
Abbreviation: TCA cycle, tricarboxylic acid cycle.

allergy only). Cellular, metabolic, and immune system processes and stimulus response were important biological processes that were modulated in response to AgNP exposure in both control and allergic mice, as determined by plasma analysis.

Pathway analysis was performed using PANTHER (Figure 5). Three pathways – blood coagulation, T-cell activation, and plasminogen activating cascade – were determined based on the AgNP-unique proteins in control groups. Notably, blood coagulation was only found in the allergy group.

Functional pathway analyses of BALF and plasma proteins

To determine the common proteins induced by AgNP exposure in control and allergy groups, the unique AgNP-associated proteins in BALF (Figure 3E) and serum (Figure 3F) were compared. There were 18 overlapping proteins in BALF (Table 1): apolipoprotein E, myosin light polypeptide 6, heterogeneous nuclear ribonucleoproteins A2/B1, transitional endoplasmic reticulum ATPase, Ig alpha chain C region, Ig heavy chain V region MOPC 47A, Ig heavy chain V region 441, histone H4, glyoxalase domain-containing protein 4, extracellular superoxide dismutase (Cu-Zn), Ig lambda-1 chain C region, annexin A2, inter-alpha-trypsin inhibitor heavy chain H2, myosin regulatory light polypeptide 9, histone H2A type 1-F, heat shock 70 kDa protein 4, vimentin, and proteasome subunit alpha type-1. Further, there were four overlapping proteins in plasma (Table 1): carboxypeptidase N subunit 2, zinc-alpha-2-glycoprotein, vasohibin-1, and interleukin-1 receptor accessory protein.

DAVID analysis revealed functional classifications, including heterotetramer ($P = 3.9 \times 10^{-5}$; 27%), immunoglobulin v region ($P = 7.7 \times 10^{-4}$; 20%), acetylation ($P = 9.4 \times 10^{-4}$; 53%), immunoglobulin ($P = 9.5 \times 10^{-4}$; 20%), immunoglobulin domain ($P = 4.5 \times 10^{-3}$; 27%), immunoglobulin c region ($P = 8.6 \times 10^{-3}$; 13%), phosphoprotein ($P = 7.9 \times 10^{-2}$; 60%), duplication ($P = 9 \times 10^{-2}$; 13%) and secretion ($P = 9.4 \times 10^{-2}$; 27%). Further, the overlapping unique AgNP-associated proteins were associated with systemic lupus erythematosus ($P = 6.8 \times 10^{-3}$; 13%). For the plasma samples, analysis of functional classification showed that the overlapping unique AgNP-associated

Table 1 Silver nanoparticle-unique proteins expressed in mice sensitized with phosphate-buffered saline (control) or ovalbumin (allergy)

No	Name of protein with UniProt accession number	Mascot* score	Calculated Mw (Dalton)	Sequence covered %	Calculated pI
BALF					
1	Apolipoprotein E (P08226)	134	35,901	12.9	5.56
2	Myosin light polypeptide 6 (P60660)	91	17,090	16.6	4.56
3	Heterogeneous nuclear ribonucleoproteins A2/B1 (O88569)	89	37,437	6.2	8.97
4	Transitional endoplasmic reticulum ATPase (P55072)	78	89,950	4.6	5.14
5	Ig alpha chain C region (P01878)	69	37,594	4.4	4.97
6	Ig heavy chain V region MOPC 47 A (P01786)	60	13,081	13.7	8.99
7	Ig heavy chain V region 441 (P01806)	56	13,074	13.8	8.46
8	Histone H4 (P20671)	56	11,360	9.7	11.36
9	Glyoxalase domain-containing protein 4 (Q9CPV4)	51	33,581	6.0	5.28
10	Extracellular superoxide dismutase (Cu-Zn) (O09164)	50	27,717	5.6	6.36
11	Ig lambda-1 chain C region (P01843)	49	11,739	32.4	5.87
12	Annexin A2 (P07356)	48	38,937	3.2	7.55
13	Inter-alpha-trypsin inhibitor heavy chain H2 (Q61703)	48	106,261	1.6	6.82
14	Myosin regulatory light polypeptide 9 (Q9CQ19)	47	19,898	5.2	4.80
15	Histone H2A type 1-F (Q8CGP5)	45	14,153	6.9	11.05
16	Heat shock 70 kDa protein 4 (Q61316)	42	94,872	1.7	5.15
17	Vimentin (P20152)	36	53,712	2.4	5.06
18	Proteasome subunit alpha type-1 (Q9R1P4)	36	29,813	4.9	6.00
Plasma					
1	Carboxypeptidase N subunit 2 (Q9DBB9)	61	61,296	2.9	5.53
2	Zinc-alpha-2-glycoprotein (Q64726)	45	35,538	5.9	5.83
3	Vasohibin-1 (Q8C1W1)	32	42,020	2.9	9.42
4	Interleukin-1 receptor accessory protein (Q61730)	31	66,383	1.8	7.85

Notes: Eighteen proteins in bronchoalveolar lavage fluid (BALF) and four proteins in plasma were identified. *Matrix Science, Boston, MA, USA.
Abbreviation: Ig, immunoglobulin.

proteins were secreted peptides ($P = 5 \times 10^{-4}$; 100%) and signaling molecules ($P = 7.2 \times 10^{-2}$; 75%). However, there was no pathway identified by these overlapping unique AgNP-associated proteins in plasma.

Determination of OVA-specific IgE

AgNP inhalation induced significant allergic responses in both control and allergy groups, as determined by the plasma levels of OVA-specific IgE in samples collected 2 days after OVA challenge ($P < 0.05$, Figure 6). There was no significant difference in the plasma levels of OVA-specific IgE in control and allergy groups before and after FA exposure. OVA-specific IgE levels were 1.3 times higher in control mice and 14.3 times higher in allergic mice after AgNP exposure.

Discussion

BALF and plasma are important biological fluids containing diverse proteins released by dysfunctional cells and injured tissues. BALF and plasma proteomics are of considerable interest for toxicological and clinical studies, particularly in disease biomarker discovery.[22,23] A "protein biomarker" is a protein or peptide that can be objectively and quantitatively measured and evaluated as an indicator of normal or pathological biological processes or exposure to environmental factors. This study used proteomics to determine the allergenicity of AgNPs, generated using the evaporation–condensation method, in allergen provoked murine models. We found 106 and 79 unique AgNP-associated proteins in BALF from control and allergic mice, respectively, after AgNP inhalation. Additionally, 40 and 26 unique AgNP-associated proteins were found in the plasma of control and allergic mice, respectively. The BALF and plasma protein profiles suggested that metabolic, cellular, and immune system processes were modulated in response to AgNP pulmonary exposure. The inhaled AgNPs may regulate immune responses in the lungs of control and allergic mice, as the overlapping unique AgNP-associated proteins in BALF (18 proteins) have also been associated with systemic lupus erythematosus. Further, significant allergy responses were observed after AgNP exposure in control and allergic mice, as determined by OVA-specific IgE.

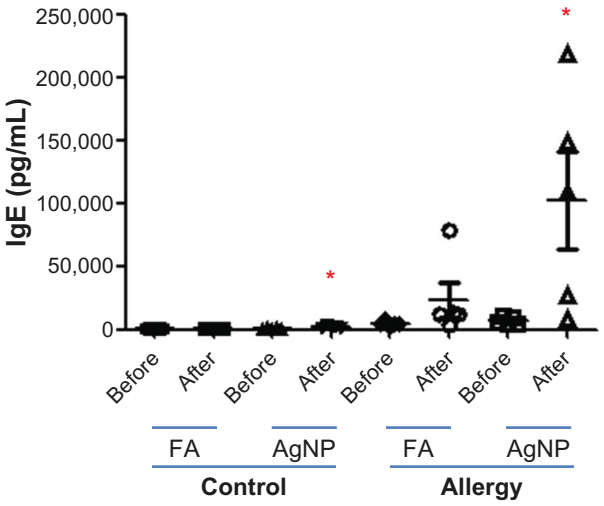

Figure 6 Ovalbumin (OVA)-specific immunoglobulin (Ig) E was collected from control and allergic mice 1 day before and 2 days after silver nanoparticle (AgNP)/filtered air (FA) inhalation and OVA challenge.
Note: Values are expressed as the means ± standard deviation; n = 5–6. *$P < 0.05$.

We investigated the allergenicity of AgNPs in the lungs of mice. The pulmonary toxicity of airborne materials is commonly evaluated by inhalation exposure in animals. These models mimic the natural route of entry into the host and, as such, are the preferred method for the introduction of toxicants into the lungs.[24] Toxicokinetics and inhalation studies are important methods used to measure the hazards associated with AgNP exposure. In this study, AgNPs were produced by the evaporation–condensation method, and the allergic responses in mice after AgNP inhalation were determined. The advantage of this procedure is that AgNPs can be generated continuously and stably for long-term inhalation at a range of levels, reflecting the natural exposure route for respirable NPs rather than exposure via intratracheal instillation or pulmonary aspiration. Pure silver powder was evaporated at 1,100°C and the vapor was quenched immediately, resulting in spherical AgNPs. Using SEM and ICP-MS, uncontaminated spherical AgNPs were generated by this method. Our results are in line with those of a previous study,[25] suggesting that the AgNPs could associate with physically bonded (ie, agglomerate) and chemically or sinter-bonded (aggregate) structures. The AgNP aggregate, with a size of 33 nm, was easily inhaled deep into the lungs and interacted with the epithelial cells.

Proteomic analyses of biological fluids are very effective for studying pathogen- or other stimulus-induced alterations in hosts and to host responses.[26] We investigated the protein profiles in BALF and plasma after AgNP inhalation by healthy (control) and diseased (OVA-sensitized allergy) mouse models. The gas-phase fractionation method was used to increase proteome coverage and the reproducibility of peptide ion selection by direct MS analysis of the peptides produced by proteolytic digestion of unfractionated proteins from the BALF and plasma samples.[8,10] Using the gas-phase fractionation method, we demonstrated that AgNPs

induced expression of 106 unique proteins in healthy mice and 79 unique proteins in OVA-sensitized mice. Protein identifications have been published previously.[8,27] Inhaled NPs first interact with the lung epithelial lining fluid, which induces a rapid biological response. PANTHER analysis identified four major biological processes associated with AgNP exposure in the BALF of control and allergic mice: metabolic, cellular, and immune system processes and cell communication. A previous study exposed Sprague Dawley rats in whole-body exposure chambers to environmental cigarette smoke for 28 days. Environmental cigarette smoke stimulated 56 proteins in lung tissues, including those involved in the stress response, protein removal, cell replication, apoptosis, phagocytosis, and the immune response.[28] A recent study observed that AgNPs have significant immunological adjuvant effects in BALB/c mice.[5] Additionally, Kang et al[29] demonstrated that ultrafine ambient particles are adjuvants that enhance allergic inflammation in BALB/c mice. Expression of polymeric immunoglobulin receptor, complement C3, neutrophil gelatinase-associated lipocalin, chitinase 3-like protein 3, chitinase 3-like protein 4, and acidic mammalian chitinase was altered in BALF after particle exposure. To compare the differences in biological processes after pulmonary exposure to AgNPs and ambient particles, in the current study, these six BALF proteins were further analyzed with PANTHER. We found that ambient particle exposure induced proteins involved in reproduction (7.7%), stimulus response (15.4%), immune system processes (15.4%), cellular processes (15.4%), metabolic processes (15.4%), cell communication (7.7%), system processes (7.7%), and transport (15.4%). A similarity was observed in the biological processes induced by AgNP exposure and ambient particle exposure. Taken together, these data suggest that pulmonary exposure to particulate substances such as AgNPs induced immune responses. The particle's physicochemistry may be a pivotal parameter that determines the severity of immunotoxicology. The physicochemical characteristics of nanoscaled particles contribute to oxidative-inflammatory reactions.[30,31] We also elucidated the functions of proteins modulated in response to AgNPs in the lung environment; these functional categories included blood coagulation, activation of the integrin signaling pathway and ubiquitin proteasome pathway; inflammation mediation by chemokines; activation of the cytokine signaling pathway; T-cell activation; activation of the tricarboxylic acid cycle, dopamine receptor-mediated signaling pathway, plasminogen activating cascade, and Fas signaling pathway; cytoskeletal regulation by Rho GTPase; and activation of the nicotine pharmacodynamics pathway and nicotinic acetylcholine receptor signaling pathway. AgNP exposure may alter blood coagulation via platelet activation and thrombus formation,[32] oxidative-inflammatory responses,[2,3] and innate immune responses.[33] The mechanisms underlying AgNP-induced pathologies should be investigated.

Additionally, we identified 40 and 26 AgNP-associated proteins in plasma from healthy and allergen-sensitized mice, respectively. PANTHER analysis indicated that the biological processes involved were similar to those in BALF samples, which were categorized as cellular, metabolic, and immune system processes and stimulus responses. Stimulus responses were the major difference between the BALF and plasma samples. Internal and external stimuli can induce biological responses. Previous studies revealed that the inhalation of AgNPs induced oxidative stress and inflammation.[3,7] AgNPs initiate oxidative imbalance in the form of inflammatory responses. Oxidative stress promotes the influx of inflammatory cells (eg, macrophages and neutrophils) to the lungs, leading to a second wave of systemic oxidative stress and inflammation due to the large quantities of free radicals released from activated inflammatory cells.[34] Blood coagulation, T-cell activation, and the plasminogen-activating cascade were associated with AgNP inhalation. Comparisons between BALF and plasma proteins suggest that because the lung environment interacts directly with inhaled AgNPs, it is important for initiating several biological pathways. In contrast, plasma samples may represent downstream biological responses to lung stimulation. The association between pulmonary and systemic responses to AgNP exposure requires further investigation.

Alterations in overlapping AgNP-associated proteins in BALF and plasma were also examined. The identified proteins were able to elucidate the common biological processes and pathways in control and allergy subjects. Further, these proteins may be candidates for AgNP-related biomarkers. Our proteomic analysis revealed 18 overlapping proteins in the BALF and four overlapping proteins in plasma. DAVID functional classification software was used to determine the pathway of the proteins identified in BALF and plasma. The proteins found in BALF samples suggest that AgNP exposure is associated with "systemic lupus erythematosus," which is an autoimmune disease characterized by intense polyclonal production of autoantibodies and circulating immune complexes. Environmental pollutants are risk factors for systemic lupus erythematosus. Cigarette smoke, for example, is positively associated with increased risk

for systemic lupus erythematosus.[35] Air pollution has been shown to be associated with autoimmune rheumatic disease in humans.[36] Systemic lupus erythematosus is characterized by a Th2 immune response[37] and increased IgE production and is also associated with allergy.[37] In this study, we observed that OVA-specific IgE levels were significantly increased following AgNP inhalation in control and allergy groups. While these results confirm that immune responses are induced by AgNP exposure, they might also suggest that exposure to AgNPs increases the risk of systemic lupus erythematosus, but this hypothesis requires further investigation.

Conclusion

Our knowledge of the mechanisms underlying asthma is still limited. As far as we are aware, this study is the first to investigate BALF and plasma protein profiles after pulmonary exposure to AgNPs. Comprehensive proteomic analysis using the gas-phase fractionation method and bioinformatics analyses revealed that several proteins were induced in the BALF and plasma of healthy and allergic mice. Our results suggest that these proteins are associated with various essential physiological processes and biological functions. Further, the BALF proteomic results suggest that immunotoxicology is a pivotal response to AgNPs. One limitation of this study is that the levels of specific proteins were not determined, and these data should be generated in future studies. We suggest that BALF proteomic profiling could be used as an effective approach to screen AgNP adjuvant effects. Our findings may fill the gap between epidemiological and clinical research, but the safety of AgNPs in airway therapeutic strategies should be examined carefully before commercial applications are implemented.

Acknowledgments

The authors wish to thank Drs Yuan-Horng Yan, Kuo-Liang Huang, Hui-Hsien Chang, and Ta-Chih Hsiao for their technical assistance with this research.

Funding

This research was a collaboration between Taipei Medical University, Shuang Ho Hospital, and the National Taiwan University. Portions of this work were performed and funded by the Shang Ho Hospital (102 SHH-HCP-16) and Taipei Medical University (grant number TMU101-AE1-B53). Some of the experimental works were performed in the National Taiwan University and supported by the National Science Council of Taiwan (grant number 101-2621-M-002-004).

Authors' contributions

All authors have contributed substantially to the concept, design, drafting the article, and critically revising the manuscript for important intellectual content. All authors read and approved the final version of the manuscript for publication.

Disclosure

The authors declare no conflicts of interest in this work.

References

1. Benn TM, Westerhoff P. Nanoparticle silver released into water from commercially available sock fabrics. *Environ Sci Technol*. 2008;42(11):4133–4139.
2. Park HS, Kim KH, Jang S, et al. Attenuation of allergic airway inflammation and hyperresponsiveness in a murine model of asthma by silver nanoparticles. *Int J Nanomedicine*. 2010;5:505–515.
3. Jang S, Park JW, Cha HR, et al. Silver nanoparticles modify VEGF signaling pathway and mucus hypersecretion in allergic airway inflammation. *Int J Nanomedicine*. 2012;7:1329–1343.
4. Foldbjerg R, Olesen P, Hougaard M, Dang DA, Hoffmann HJ, Autrup H. PVP-coated silver nanoparticles and silver ions induce reactive oxygen species, apoptosis and necrosis in THP-1 monocytes. *Toxicol Lett*. 2009;190(2):156–162.
5. Xu Y, Tang H, Liu JH, Wang H, Liu Y. Evaluation of the adjuvant effect of silver nanoparticles both in vitro and in vivo. *Toxicol Lett*. 2013;219(1):42–48.
6. Ghosh M, J M, Sinha S, et al. In vitro and in vivo genotoxicity of silver nanoparticles. *Mutat Res*. 2012;749(1–2):60–69.
7. Mei N, Zhang Y, Chen Y, et al. Silver nanoparticle-induced mutations and oxidative stress in mouse lymphoma cells. *Environ Mol Mutagen*. 2012;53(6):409–419.
8. Yu CJ, Wang CL, Wang CI, et al. Comprehensive proteome analysis of malignant pleural effusion for lung cancer biomarker discovery by using multidimensional protein identification technology. *J Proteome Res*. 2011;10(10):4671–4682.
9. Schrohl AS, Würtz S, Kohn E, et al. Banking of biological fluids for studies of disease-associated protein biomarkers. *Mol Cell Proteomics*. 2008;7(10):2061–1066.
10. Yi EC, Marelli M, Lee H, et al. Approaching complete peroxisome characterization by gas-phase fractionation. *Electrophoresis*. 2002;23(18):3205–3216.
11. Kennedy J, Yi EC. Use of gas-phase fractionation to increase protein identifications: application to the peroxisome. *Methods Mol Biol*. 2008;432:217–228.
12. Brook RD, Rajagopalan S, Pope CA III, et al. Particulate matter air pollution and cardiovascular disease: An update to the scientific statement from the American Heart Association. *Circulation*. 2010;121(21):2331–2378.
13. Ho M, Wu KY, Chein HM, Chen LC, Cheng TJ. Pulmonary toxicity of inhaled nanoscale and fine zinc oxide particles: mass and surface area as an exposure metric. *Inhal Toxicol*. 2011;23(14):947–956.
14. Singh Y, Javier RN, Ehrman SH, Magnusson M, Deppert K. Approaches to increasing yield in evaporation/condensation nanoparticle generation. *J Aerosol Sci*. 2002;33(9):1309–1325.
15. Maciejczyk P, Zhong M, Li Q, Xiong J, Nadziejko C, Chen LC. Effects of subchronic exposures to concentrated ambient particles (CAPs) in mice. II. The design of a CAPs exposure system for biometric telemetry monitoring. *Inhal Toxicol*. 2005;17(4–5):189–197.
16. Moreno T, Gibbons W, Jones T, Richards R. The geology of ambient aerosols: characterising urban and rural/coastal silicate $PM_{10-2.5}$ and $PM_{2.5}$ using high-volume cascade collection and scanning electron microscopy. *Atmos Environ*. 2003;37(30):4265–4276.

17. Jones T, Moreno T, BéruBé K, Richards R. The physicochemical characterisation of microscopic airborne particles in south Wales: a review of the locations and methodologies. *Sci Total Environ*. 2006;360(1–3):43–59.
18. Pichavant M, Goya S, Hamelmann E, Gelfand EW, Umetsu DT. Animal models of airway sensitization. *Curr Protoc Immunol*. 2007;Chapter 15:Unit 15.18.
19. Li N, Wang M, Bramble LA, et al. The adjuvant effect of ambient particulate matter is closely reflected by the particulate oxidant potential. *Environ Health Perspect*. 2009;117(7):1116–1123.
20. Huang da W, Sherman BT, Tan Q, et al. DAVID Bioinformatics resources: expanded annotation database and novel algorithms to better extract biology from large gene lists. *Nucleic Acids Res*. 2007;35(Web Server issue):W169–W175.
21. Srivastava R, Ray S, Vaibhav V, et al. Serum profiling of leptospirosis patients to investigate proteomic alterations. *J Proteomics*. 2012;76 Spec No:56–68.
22. Sul D. Evaluation of toxicological monitoring markers using proteomic analysis. *J Proteome Res*. 2006;5(10):2525–2526.
23. Kennedy S. The role of proteomics in toxicology: identification of biomarkers of toxicity by protein expression analysis. *Biomarkers*. 2002;7(4):269–290.
24. Driscoll KE, Costa DL, Hatch G, et al. Intratracheal instillation as an exposure technique for the evaluation of respiratory tract toxicity: uses and limitations. *Toxicol Sci*. 2000;55(1):24–35.
25. Eggersdorfer ML, Kadau D, Herrmann HJ, Pratsinis SE. Aggregate morphology evolution by sintering: number and diameter of primary particles. *J Aerosol Sci*. 2012;46:7–19.
26. Gharib SA, Nguyen EV, Lai Y, Plampin JD, Goodlett DR, Hallstrand TS. Induced sputum proteome in healthy subjects and asthmatic patients. *J Allergy Clin Immunol*. 2011;128(6):1176–1184. e6.
27. Tyan YC, Wu HY, Lai WW, Su WC, Liao PC. Proteomic profiling of human pleural effusion using two-dimensional nano liquid chromatography tandem mass spectrometry. *J Proteome Res*. 2005;4:1274–1286.
28. Izzotti A, Bagnasco M, Cartiglia C, et al. Chemoprevention of genome, transcriptome, and proteome alterations induced by cigarette smoke in rat lung. *Eur J Cancer*. 2005;41(13):1864–1874.
29. Kang X, Li N, Wang M, et al.Adjuvant effects of ambient particulate matter monitored by proteomics of bronchoalveolar lavage fluid. *Proteomics*. 2010;10: 520–531.
30. Chuang HC, Cheng YL, Lei YC, Chang HH, Cheng TJ. Protective effects of pulmonary epithelial lining fluid on oxidative stress and DNA single-strand breaks caused by ultrafine carbon black, ferrous sulphate and organic extract of diesel exhaust particles. *Toxicol Appl Pharmacol*. 2013;266(3):329–334.
31. Chuang HC, Fan CW, Chen KY, Chang-Chien GP, Chan CC. Vasoactive alteration and inflammation induced by polycyclic aromatic hydrocarbons and trace metals of vehicle exhaust particles. *Toxicol Lett*. 2012;214:131–136.
32. Jun EA, Lim KM, Kim K, et al. Silver nanoparticles enhance thrombus formation through increased platelet aggregation and procoagulant activity. *Nanotoxicology*. 2011;5(2):157–167.
33. Bezemer GF, Bauer SM, Oberdörster G, et al. Activation of pulmonary dendritic cells and Th2-type inflammatory responses on instillation of engineered, environmental diesel emission source or ambient air pollutant particles in vivo. *J Innate Immun*. 2011;3(2):150–166.
34. Kelly FJ. Oxidative stress: its role in air pollution and adverse health effects. *Occup Environ Med*. 2003;60(8):612–616.
35. Kiyohara C, Washio M, Horiuchi T, et al. Cigarette smoking, alcohol consumption, and risk of systemic lupus erythematosus: a case-control study in a Japanese population. *J Rheumatol*. 2012;39(7):1363–1370.
36. Bernatsky S, Fournier M, Pineau CA, Clarke AE, Vinet E, Smargiassi A. Associations between ambient fine particulate levels and disease activity in patients with systemic lupus erythematosus (SLE). *Environ Health Perspect*. 2011;119(1):45–49.
37. Atta AM, Sousa CP, Carvalho EM, Sousa-Atta ML. Immunoglobulin E and systemic lupus erythematosus. *Braz J Med Biol Res*. 2004;37(10):1497–1501.

Supplementary tables

The following tables present the protein profiles in BALF and plasma that do not appear in the main part of the article.

Table S1 Silver nanoparticle-unique proteins expressed in bronchoalveolar lavage fluid in the control mice

No	Name of protein	Mascot* score	Calculated Mw (Dalton)	Sequence covered %	Calculated pI
1	Polymeric immunoglobulin receptor	775	86,257	15.3	5.26
2	Serine protease inhibitor A3N	650	46,859	18.4	5.59
3	Fibronectin	243	276,017	3.7	5.39
4	Ig kappa chain C region	218	11,942	13.2	5.23
5	Histone H4	173	11,360	21.4	11.36
6	Fatty acid-binding protein, adipocyte	159	14,755	9.8	8.53
7	Ig heavy chain V region MOPC 47A	125	13,081	23.1	8.99
8	Heat shock 70 kDa protein 4	122	94,872	3.3	5.15
9	Resistin-like alpha	117	12,612	13.5	5.18
10	Myosin-9	107	227,429	1.7	5.54
11	Extracellular superoxide dismutase (Cu-Zn)	105	27,717	10.8	6.36
12	Histone H2A type 1-F	101	14,153	22.3	11.05
13	Properdin	100	52,802	7.1	8.25
14	Complement component C8 alpha chain	94	67,691	6.1	6.14
15	Ig heavy chain V region 441	93	13,074	33.6	8.46
16	Protein Z-dependent protease inhibitor	84	51,878	2.7	5.49
17	Tubulin alpha-1A chain	80	50,788	4.4	4.94
18	Proteasome subunit alpha type-6	78	27,811	5.3	6.34
19	Ig lambda-1 chain C region	76	11,739	16.2	5.87
20	Proteasome subunit alpha type-3	76	28,615	4.7	5.29
21	Proteasome subunit beta type-8	73	30,526	9.1	6.22
22	Cathepsin B	73	38,168	7.1	5.57
23	Fibrinogen gamma chain	72	50,044	5.5	5.54
24	Complement factor H	69	143,722	1.0	6.67
25	Transitional endoplasmic reticulum ATPase	69	89,950	1.5	5.14
26	CD177 antigen	69	90,284	1.3	5.43
27	Peptidyl-prolyl cis-trans isomerase B	68	23,699	6.0	9.56
28	SUMO-activating enzyme subunit 1	68	39,052	3.4	5.24
29	Annexin A2	66	38,937	6.5	7.55
30	Intercellular adhesion molecule 1	65	59,605	2.6	5.79
31	Ig alpha chain C region	65	37,594	4.4	4.97
32	Interleukin-1 receptor accessory protein	63	66,383	1.9	7.85
33	Myosin light polypeptide 6	63	17,090	16.6	4.56
34	Alpha-actinin-4	63	105,368	3.2	5.25
35	Isocitrate dehydrogenase (NADP), mitochondrial	63	51,330	2.9	8.88
36	Keratin, type II cytoskeletal 1	62	66,079	1.7	8.39
37	Keratin, type II cytoskeletal 2 epidermal	61	71,336	2.0	8.26
38	Microsomal glutathione S-transferase 1	59	17,597	8.4	9.67
39	Vimentin	59	53,712	2.4	5.06
40	Alpha/beta hydrolase domain-containing protein 14B	58	22,551	6.7	5.82
41	Dipeptidyl peptidase 1	58	53,141	2.6	6.41
42	Heterogeneous nuclear ribonucleoproteins A2/B1	58	37,437	2.8	8.97
43	Brain acid soluble protein 1	56	22,074	6.2	4.50
44	60S acidic ribosomal protein P0	56	34,366	3.5	5.91
45	Transforming growth factor-beta-induced protein ig-h3	56	75,177	2.0	6.62
46	Glutathione reductase, mitochondrial	55	54,256	2.6	8.19
47	Ig heavy chain V region MOPC 104E	54	13,089	16.2	6.84
48	Proteasome assembly chaperone 1	53	33,938	4.8	6.05
49	Apolipoprotein E	52	35,901	8.7	5.56
50	Alpha-2-antiplasmin	52	55,165	2.9	5.85

(*Continued*)

Table S1 (*Continued*)

No	Name of protein	Mascot* score	Calculated Mw (Dalton)	Sequence covered %	Calculated pI
51	Ig heavy chain V-III region J606	52	12,916	11.3	6.86
52	Phosphoglucomutase-1	52	61,665	2.1	6.14
53	Proteasome subunit alpha type-1	51	29,813	4.9	6.00
54	Growth arrest-specific protein 6	50	76,500	1.8	5.34
55	Poly(rC)-binding protein 1	49	37,987	3.1	6.66
56	Hepatocyte growth factor activator	49	72,860	2.6	6.65
57	Epididymal secretory protein E1	48	16,774	8.1	7.59
58	Na(+)/H(+) exchange regulatory cofactor NHE-RF1	48	38,862	3.9	5.63
59	Complement C2	45	85,942	1.6	7.52
60	Plasma protease C1 inhibitor	45	55,834	2.2	5.87
61	Peptidoglycan recognition protein 1	45	20,875	6.6	7.07
62	Small glutamine-rich tetratricopeptide repeat-containing protein alpha	45	34,529	4.1	4.99
63	Leukemia inhibitory factor receptor	44	123,808	1.2	5.70
64	Lamin-B1	43	66,973	2.4	5.11
65	Nuclease-sensitive element-binding protein 1	42	35,709	4.7	9.87
66	LIM and SH3 domain protein 1	42	30,374	4.9	6.61
67	Cathepsin Z	42	34,658	3.6	6.13
68	C-C motif chemokine 6	42	13,318	9.5	9.50
69	Myosin regulatory light polypeptide 9	40	19,898	5.8	4.80
70	60S ribosomal protein L7	40	31,457	4.8	10.89
71	Tetranectin	39	22,642	6.9	5.50
72	Chloride intracellular channel protein 5	38	28,440	4.8	5.64
73	Aminopeptidase N	38	110,038	1.3	5.62
74	Thyroglobulin	38	311,291	0.4	5.32
75	Ribonuclease 4	37	17,470	8.1	9.18
76	Pulmonary surfactant-associated protein C	37	21,269	9.3	6.42
77	Cystatin-C	37	15,749	11.4	9.18
78	Epidermal growth factor receptor	37	138,187	1.5	6.46
79	Glyoxylate reductase/hydroxypyruvate reductase	37	35,706	3.7	7.57
80	LIM and calponin homology domains-containing protein 1	37	119,035	1.2	5.38
81	Myeloperoxidase	37	82,042	1.5	9.63
82	Cell division cycle protein 27 homolog	36	92,868	1.5	6.59
83	Carbonic anhydrase 6	36	36,586	3.8	6.11
84	Lumican	36	38,640	3.3	6.00
85	Zinc-alpha-2-glycoprotein	35	35,538	5.9	5.83
86	Calreticulin	35	48,136	3.1	4.33
87	Kinesin-1 heavy chain	34	110,225	1.7	6.06
88	Inter-alpha-trypsin inhibitor heavy chain H2	33	106,261	1.3	6.82
89	Glucosidase 2 subunit beta	33	59,725	2.3	4.41
90	Ubiquitin carboxyl-terminal hydrolase 5	33	96,685	1.5	4.89
91	Sulfhydryl oxidase 1	33	83,531	1.7	6.73
92	Lysozyme C-1	33	17,240	8.1	9.55
93	Ubiquitin carboxyl-terminal hydrolase 14	33	56,422	2.8	5.15
94	EF-hand domain-containing protein D2	32	26,775	5.0	5.01
95	Lymphocyte-specific protein 1	32	36,806	3.9	4.77
96	Hepatoma-derived growth factor	32	26,367	8.4	4.80
97	Aspartyl aminopeptidase	32	52,744	3.0	6.82
98	Glyoxalase domain-containing protein 4	32	33,581	5.0	5.28
99	Fatty acid synthase	32	274,994	0.4	6.13
100	Dihydropyrimidinase-related protein 1	32	62,471	2.8	6.63
101	Nuclear migration protein nudC	31	38,334	3.3	5.17
102	Tax1-binding protein 3	31	13,714	13.7	8.04
103	Inter-alpha-trypsin inhibitor, heavy chain 4	31	104,765	1.5	5.99
104	Complement factor I	31	69,497	2.5	7.57
105	Von Willebrand factor A domain-containing protein 5A	31	87,829	1.5	6.15
106	Vomeromodulin	30	62,751	2.0	5.46

Note: *Matrix Science, Boston, MA, USA.

Abbreviations: CD, cluster of differentiation; Ig, immunoglobulin; NADPH, nicotinamide adenine dinucleotide phosphate; SUMO, small ubiquitin-like modifier.

Table S2 Silver nanoparticle-unique proteins expressed in bronchoalveolar lavage fluid in the allergy mice

No	Name of protein	Mascot* score	Calculated Mw (Dalton)	Sequence covered %	Calculated pI
1	Actin, aortic smooth muscle	523	42,381	22.3	5.23
2	Glutathione peroxidase 3	179	25,580	15.0	8.33
3	Protein S100-A9	174	13,211	23.0	6.64
4	BPI fold-containing family A member 1	169	28,778	6.8	6.02
5	Fibrinogen beta chain	150	55,402	9.8	6.68
6	Nucleoside diphosphate kinase B	143	17,466	28.3	6.97
7	Apolipoprotein E	134	35,901	12.9	5.56
8	Serpin B6	133	42,913	6.6	5.53
9	Ig heavy chain V-III region A4	116	12,781	22.1	7.00
10	ADP-ribosylation factor 1	109	20,741	14.4	6.32
11	Myosin light polypeptide 6	91	17,090	16.6	4.56
12	Ig gamma-3 chain C region	90	44,472	2.0	6.68
13	Heterogeneous nuclear ribonucleoproteins A2/B1	89	37,437	6.2	8.97
14	Ig kappa chain V-V region K2 (Fragment)	89	12,744	8.7	8.50
15	Advanced glycosylation end product-specific receptor	80	42,984	5.2	5.78
16	Transitional endoplasmic reticulum ATPase	78	89,950	4.6	5.14
17	Creatine kinase M-type	74	43,246	7.9	6.58
18	CD5 antigen-like	71	40,320	6.3	5.01
19	Ig heavy chain V region 93G7	70	15,619	7.1	8.50
20	Ig alpha chain C region	69	37,594	4.4	4.97
21	Carbonic anhydrase 3	68	29,633	8.1	6.89
22	Myotrophin	64	13,024	14.4	5.27
23	Ig kappa chain V-V region L7 (Fragment)	61	12,721	10.4	5.63
24	Tropomyosin beta chain	61	32,931	7.7	4.66
25	Ig heavy chain V region MOPC 47A	60	13,081	13.7	8.99
26	Glycogenin-1	60	37,606	4.2	5.06
27	Ig kappa chain V19-17	59	16,537	6.0	6.38
28	Aminopeptidase B	57	73,054	1.5	5.22
29	Cytosolic nonspecific dipeptidase	57	53,190	2.3	5.43
30	Proteasome subunit beta type-4	56	29,211	3.8	5.47
31	Ig heavy chain V region 441	56	13,074	13.8	8.46
32	Histone H4	56	11,360	9.7	11.36
33	6-phosphogluconate dehydrogenase, decarboxylating	56	53,726	2.3	6.81
34	Keratin, type I cytoskeletal 10	55	57,906	2.8	5.04
35	Transforming protein RhoA	53	22,110	9.8	5.83
36	BPI fold-containing family B member 1	53	52,593	4.9	5.96
37	Carbonyl reductase (NADPH) 1	52	30,907	3.2	8.53
38	Glyoxalase domain-containing protein 4	51	33,581	6.0	5.28
39	Extracellular superoxide dismutase (Cu-Zn)	50	27,717	5.6	6.36
40	Ig lambda-1 chain C region	49	11,739	32.4	5.87
41	Basal cell adhesion molecule	49	68,426	2.3	5.85
42	Alcohol dehydrogenase [NADP(+)]	49	36,792	4.9	6.90
43	Myoglobin	49	17,116	11.0	7.07
44	Ig kappa chain V-II region 17S29.1	48	12,496	11.5	7.97
45	Protein S100-A11	48	11,247	7.1	5.28
46	Annexin A2	48	38,937	3.2	7.55
47	Inter-alpha-trypsin inhibitor heavy chain H2	48	106,261	1.6	6.82
48	Heterogeneous nuclear ribonucleoprotein A3	48	39,856	2.6	9.10
49	Myosin regulatory light polypeptide 9	47	19,898	5.2	4.80
50	Flavin reductase (NADPH)	47	22,297	8.3	6.49
51	Band 3 anion transport protein	46	103,412	1.0	5.31
52	Histone H3.3C	45	15,363	5.1	11.14
53	Histone H2A type 1-F	45	14,153	6.9	11.05
54	Complement C4-B	44	194,447	0.5	7.38
55	Heat shock 70 kDa protein 4	42	94,872	1.7	5.15
56	Ig lambda-2 chain C region	41	11,419	17.3	5.86

(*Continued*)

Table S2 (*Continued*)

No	Name of protein	Mascot* score	Calculated Mw (Dalton)	Sequence covered %	Calculated pI
57	Retinol-binding protein 4	40	23,533	5.0	5.69
58	Apolipoprotein A-II	39	11,359	9.8	6.56
59	Talin-1	38	271,820	0.4	5.84
60	Galectin-3	38	27,612	4.2	8.46
61	Chloride intracellular channel protein 1	38	27,338	5.0	5.09
62	Alpha-actinin-1	37	103,631	1.1	5.23
63	Vimentin	36	53,712	2.4	5.06
64	Proteasome subunit alpha type-1	36	29,813	4.9	6.00
65	L-xylulose reductase	35	25,958	4.5	6.82
66	Coronin-1B	35	54,505	1.4	5.54
67	Proteasome subunit beta type-7	35	30,214	3.6	8.14
68	Protein AMBP	35	39,916	2.9	5.96
69	Filamin-A	34	283,897	0.4	5.68
70	Alcohol dehydrogenase 1	34	40,601	1.9	8.44
71	Calmodulin	33	16,827	4.7	4.09
72	Immunoglobulin J chain	33	18,458	5.0	4.77
73	Proteasome subunit alpha type-7-like	32	28,020	4.4	8.81
74	NADPH-cytochrome P450 reductase	31	77,394	1.3	5.34
75	Cofilin-1	31	18,776	4.8	8.22
76	Thiosulfate sulfurtransferase	31	33,673	2.4	7.71
77	Leucine-rich repeat-containing protein 16A	31	153,305	0.5	7.98
78	Cofilin-2	31	18,812	4.8	7.66
79	Phosphoglycerate kinase 1	30	44,921	2.6	8.02

Note: *Matrix Science, Boston, MA, USA.
Abbreviations: AMBP, alpha-1-microglobulin/bikunin precursor; CD, cluster of differentiation; Ig, immunoglobulin; SUMO, small ubiquitin-like modifier.

Table S3 Silver nanoparticle-unique proteins expressed in plasma in the control mice

No	Name of protein	Mascot* score	Calculated Mw (Dalton)	Sequence covered %	Calculated pI
1	Alpha-1-antitrypsin 1-1	1,890	46,145	33.4	5.44
2	Apolipoprotein B-100	185	510,481	1.3	6.35
3	Complement C5	148	190,469	3.0	6.39
4	Ig heavy chain V regions TEPC 15/S107/HPCM1/ HPCM2/HPCM3	147	13,883	23.6	6.51
5	Immunoglobulin J chain	140	18,458	16.4	4.77
6	Fetuin-B	140	43,541	14.7	6.17
7	Ig kappa chain V-III region ABPC 22/PC 9245	125	12,148	30.6	4.90
8	Fructose-bisphosphate aldolase B	116	39,938	7.1	8.52
9	Keratin, type II cytoskeletal 1b	115	61,379	4.2	7.74
10	Ig kappa chain V-VI region NQ2-17.4.1	104	11,668	24.3	9.43
11	Serum amyloid A-1 protein	102	13,876	18.9	6.50
12	Carboxypeptidase N subunit 2	100	61,296	5.1	5.53
13	Lumican	88	38,640	6.2	6.00
14	Ig heavy chain V region MOPC 21 (Fragment)	83	15,232	16.2	8.83
15	Ig heavy chain V region 441	83	13,074	10.3	8.46
16	Ig heavy chain V region 5-84	79	13,035	23.1	9.05
17	Carboxypeptidase B2	71	49,239	5.5	8.03
18	Complement component C8 beta chain	68	68,011	2.2	8.07
19	Ig heavy chain V-III region A4	68	12,781	8.0	7.00
20	Complement C1q subcomponent subunit B	63	26,929	4.7	8.30
21	Flavin reductase (NADPH)	62	22,297	4.9	6.49
22	Coagulation factor XIII B chain	61	78,426	1.6	6.56
23	Interleukin-1 receptor accessory protein	56	66,383	4.2	7.85
24	Thrombospondin-1	56	133,555	1.0	4.72
25	Complement component C8 gamma chain	52	22,665	6.9	9.37

(*Continued*)

Table S3 (*Continued*)

No	Name of protein	Mascot* score	Calculated Mw (Dalton)	Sequence covered %	Calculated pI
26	Complement component C8 alpha chain	48	67,691	2.2	6.14
27	Ig kappa chain V-V region K2 (Fragment)	47	12,744	8.7	8.50
28	Vitamin K-dependent protein Z	46	45,587	3.3	5.60
29	Keratin, type II cytoskeletal 2 oral	43	63,319	1.5	8.68
30	Carboxypeptidase N catalytic chain	42	52,098	2.6	8.42
31	Nesprin-1	40	1,016,650	0.1	5.43
32	Zinc-alpha-2-glycoprotein	40	35,538	3.9	5.83
33	Fibroblast growth factor 1	39	17,578	20.0	6.52
34	Proteasome subunit beta type-6	38	25,591	4.6	4.97
35	Laminin subunit alpha-5	36	416,165	0.5	6.28
36	Immunoglobulin superfamily member 10	35	287,757	0.3	9.38
37	Ig kappa chain V-II region 7S34.1	34	12,659	11.5	8.89
38	Ig heavy chain V region 93G7	34	15,619	7.1	8.50
39	Vasohibin-1	32	42,020	2.9	9.42
40	Ig gamma-2A chain C region, A allele	31	36,936	5.8	7.23

Note: *Matrix Science, Boston, MA, USA.
Abbreviations: Ig, immunoglobulin; NADP: nicotinamide adenine dinucleotide phosphate.

Table S4 Silver nanoparticle-unique proteins expressed in plasma in the allergy mice

No	Name of protein	Mascot* score	Calculated Mw (Dalton)	Sequence covered %	Calculated pI
1	Ig alpha chain C region	157	37,594	7.3	4.97
2	Ig kappa chain V-VI region NQ2-6.1	113	11,820	14.8	8.98
3	Vitronectin	108	55,613	5.2	5.67
4	Inhibitor of carbonic anhydrase	91	78,711	3.1	7.00
5	Prothrombin	81	71,649	2.1	6.04
6	Leukemia inhibitory factor receptor	71	123,808	1.2	5.70
7	Coagulation factor X	69	55,409	4.8	5.50
8	Inter-alpha-trypsin inhibitor heavy chain H1	65	101,460	1.4	6.49
9	Carboxypeptidase N subunit 2	61	61,296	2.9	5.53
10	Ig kappa chain V-II region 17S29.1	61	12,496	11.5	7.97
11	Apolipoprotein C-IV	57	14,450	16.1	9.64
12	Plasma kallikrein	56	73,446	1.6	8.40
13	Superoxide dismutase (Cu-Zn)	56	16,104	7.8	6.02
14	Ig kappa chain V19-17	50	16,537	6.0	6.38
15	Mannose-binding protein A	48	25,836	3.8	7.55
16	Zinc-alpha-2-glycoprotein	45	35,538	5.9	5.83
17	Apolipoprotein C-II	38	10,734	9.3	4.78
18	Ig heavy chain V region B1-8/186-2	35	15,581	5.0	8.94
19	Apolipoprotein D	35	21,744	3.7	4.82
20	Prolow-density lipoprotein receptor-related protein 1	35	523,342	0.2	5.14
21	Dystrophin	33	427,676	0.3	5.66
22	Sulfhydryl oxidase 1	32	83,531	0.9	6.73
23	Betaine-homocysteine S-methyltransferase 1	32	45,448	2.5	8.01
24	Vasohibin-1	32	42,020	2.9	9.42
25	Interleukin-1 receptor accessory protein	31	66,383	1.8	7.85
26	E3 ubiquitin-protein ligase RNF123	30	150,040	0.5	6.25

Note: *Matrix Science, Boston, MA, USA.
Abbreviation: Ig, immunoglobulin.